Journal of Geophysical Research: Biogeosciences

RESEARCH ARTICLE
10.1029/2017JG004369

Flooding Alters Plant-Mediated Carbon Cycling Independently of Elevated Atmospheric CO_2 Concentrations

Scott F. Jones[1,2], Camille L. Stagg[3], Ken W. Krauss[3], and Mark W. Hester[1]

[1]Coastal Plant Ecology Lab, Department of Biology, University of Louisiana at Lafayette, Lafayette, LA, USA, [2]DeFelice Marine Center, Louisiana Universities Marine Consortium, Chauvin, LA, USA, [3]Wetland and Aquatic Research Center, U.S. Geological Survey, Lafayette, LA, USA

Key Points:
- We quantify changes in plant-mediated carbon cycling to altered hydrology and CO_2 concentrations in a blue carbon salt marsh system
- Greater average flooding depth increased plant carbon exchange and decreased the total carbon pool
- The drivers of cellulose decomposition were not constant over an extended hydrologic gradient

Supporting Information:
- Supporting Information S1

Correspondence to:
S. F. Jones,
sjones@lumcon.edu;
scott.jones90@gmail.com

Citation:
Jones, S. F., Stagg, C. L., Krauss, K. W., & Hester, M. W. (2018). Flooding alters plant-mediated carbon cycling independently of elevated atmospheric CO_2 concentrations. *Journal of Geophysical Research: Biogeosciences*, *123*, 1976–1987. https://doi.org/10.1029/2017JG004369

Received 18 DEC 2017
Accepted 29 MAY 2018
Accepted article online 8 JUN 2018
Published online 29 JUN 2018

Abstract Plant-mediated processes determine carbon (C) cycling and storage in many ecosystems; how plant-associated processes may be altered by climate-induced changes in environmental drivers is therefore an essential question for understanding global C cycling. In this study, we hypothesize that environmental alterations associated with near-term climate change can exert strong control on plant-associated ecosystem C cycling and that investigations along an extended hydrologic gradient may give mechanistic insight into C cycling. We utilize a mesocosm approach to investigate the response of plant, soil, and gaseous C cycling to changing hydrologic regimes and elevated atmospheric carbon dioxide (CO_2) concentrations expected by 2100 in a coastal salt marsh in Louisiana, USA. Although elevated CO_2 had no significant effects on C cycling, we demonstrate that greater average flooding depth stimulated C exchange, with higher rates of labile C decomposition, plant CO_2 assimilation, and soil C respiration. Greater average flooding depth also significantly decreased the soil C pool and marginally increased the aboveground biomass C pool, leading to net losses in total C stocks. Further, flooding depths along an extended hydrologic gradient garnered insight into decomposition mechanisms that was not apparent from other data. In C-4 dominated salt marshes, sea level rise will likely overwhelm effects of elevated CO_2 with climate change. Deeper flooding associated with sea level rise may decrease long-term soil C pools and quicken C exchange between soil and atmosphere, thereby threatening net C storage in salt marsh habitats. Manipulative studies will be indispensable for understanding biogeochemical cycling under future conditions.

Plain Language Summary This study examines how near-term climate change may affect the exchange and storage of carbon by plants in salt marshes. Our results indicate that sea level rise will increase the amount of carbon that is moved from the soil into the atmosphere, shrinking the amount of carbon in salt marsh soil. This may reduce the ability of salt marshes to keep carbon in soil long term and decrease the ability of salt marshes to offset climate change. As salt marshes are some of the best ecosystems on the planet for storing carbon in soils, any change in how these ecosystems process carbon is important to understand.

1. Introduction

Carbon (C) cycling is a critical ecosystem function that determines how much C is stored or sequestered in various pools (Lal, 2004; Pan et al., 2011) and how much C is released back into the atmosphere. Carbon cycling in vegetation-dominated communities is often mediated by plants, as plants assimilate and sequester carbon dioxide (CO_2), vent CO_2 and methane from soil respiration to the atmosphere (reviewed in Reddy & DeLaune, 2008), and affect rates of decomposition (Mueller et al., 2016). Because of the important roles that plants play in mediating ecological function, understanding how plant responses vary along environmental gradients is crucial for predicting how ecosystem C cycling may shift with environmental change.

Climate change is altering environmental gradients through increased atmospheric CO_2 concentrations, increased temperatures, and sea level rise (IPCC, 2013). Coastal habitats are located at the junction of marine and terrestrial biomes and thus have to respond to sea level rise and increasing atmospheric CO_2 concentrations in concert. As coastal plants respond to climate change, we expect that plant-mediated ecosystem functions, including C cycling, will respond in kind. Climate change will also increase the severity and frequency of disturbances, including drought and flooding (IPCC, 2013), that coastal systems experience. These rare events occur at the boundary of hydrologic gradients marshes are adapted to and may push ecosystems into alternative stable states (Beisner et al., 2003). Climate change may therefore indirectly impact ecosystem C cycling

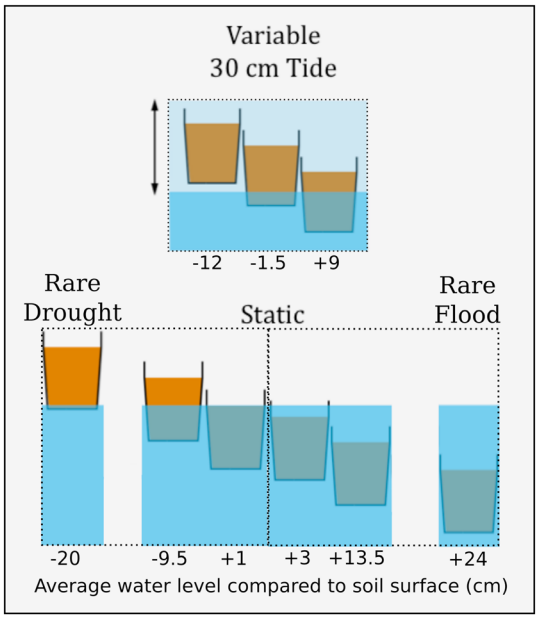

Figure 1. Experimental design showing water level and inundation type treatments. Four static and three tidal treatments experienced water levels within the in situ tidal range (−18.5 to +18.5 cm), while two static treatments experienced rare conditions (−20 and +24 cm). The dotted lines show tank groupings.

through shifts in plant community dynamics (e.g., Stagg, Schoolmaster, Krauss, et al., 2017), which may occur gradually with consistent environmental change or stochastically with rare conditions.

Salt marsh C cycling is of special global interest because of their large C storage capacity, often termed "blue carbon," that may help mitigate climate change impacts globally (Bridgham et al., 2006; Duarte et al., 2013; Mcleod et al., 2011). Salt marshes can store C-rich organic matter on millennial time scales (Chmura et al., 2003; Mitsch et al., 2013) and have the ability to increase their C storage capacity through continuous elevation gains (Morris et al., 2002; Reed, 1995). These habitats are also model systems for exploring responses of C cycling to climate change because they can exist along wide hydrologic gradients and experience rare hydrologic conditions (e.g., McKee et al., 2004). Rare conditions are difficult to capture in the field, but understanding C cycling along an extended hydrologic gradient may give insight into the mechanisms behind key processes.

Despite an increase in studies investigating C cycling in coastal salt marshes, uncertainty remains in how C cycling will respond to sea level rise and elevated atmospheric CO_2 concentrations expected in the next century (Hopkinson et al., 2012; Mcleod et al., 2011). There is conflicting evidence in the literature on how key pieces of the C cycle, such as decomposition, respond to sea level rise (Kirwan et al., 2013; Mueller et al., 2016; Stagg, Schoolmaster, Krauss, et al., 2017). Hydrologic gradient analyses have elucidated C-related responses for typical conditions, but few studies have captured responses to rare conditions on the edge of the hydrologic gradient (e.g., Zedler et al., 1986). Incorporating variability in hydrologic treatments along an extended gradient that includes rare conditions may be crucial to generating realistic stress responses, as in temperature experiments (Thompson et al., 2013). Few studies have investigated salt marsh C cycling responses to CO_2 concentrations in marshes dominated by C-4 photosynthetic pathway plants (Cherry et al., 2009; McKee & Rooth, 2008), as manipulating CO_2 concentrations is costly and logistically difficult. C-4 dominated marshes may not show direct responses to CO_2 concentrations, but indirect effects from enhanced water-use efficiency may be important drivers of C cycling in these marshes (Sage & Kubien, 2003). Further, marsh plant responses to CO_2 concentrations may be influenced by other co-occurring drivers such as increased nitrogen loads and sea level rise (e.g., Erickson et al., 2007; Langley & Megonigal, 2010). Understanding how C cycling responds to changing conditions in salt marshes allows insight into how alterations in environmental gradients associated with climate change may shift C cycling in ecosystems more generally.

We investigated how changes in atmospheric carbon dioxide concentration and average water depth associated with near-term (before 2100) climate change may alter the C cycling of *Spartina alterniflora* dominated coastal salt marsh and included rare treatments along an extended hydrologic gradient. We hypothesized that (1) hydrologic regime would be the dominant driver of C cycling in this C-4 marsh; (2) the amount of C exchanged through the system would mirror trends in plant production, with high turnover rates associated with high production; and (3) simulated sea level rise would stimulate the amount of C stored in biomass and soil pools up to a flooding stress threshold, after which C pools would decrease due to plant stress.

2. Materials and Methods

We manipulated carbon dioxide concentrations and hydrologic regimes to represent near-term climate conditions in a controlled greenhouse environment, using mesocosms of *S. alterniflora*. Hydrologic regimes represented both static and tidal inundation and included conditions that are rarely observed in the field to encompass the entire hydrologic gradient these marshes experience (Figure 1). In response to these treatments, we measured a suite of C cycling parameters, including C stored in biomass and soil pools, assimilation of carbon dioxide into plant tissue, emission of C gases from plants and soil, and decomposition of labile C in soils. We utilized a mixed model framework to analyze the nested design.

2.1. Experimental Design

In early summer 2014, we collected sods of intact soil and vegetation from monospecific stands of *S. alterniflora* in southeastern Louisiana, United States (29.18°N, 90.25°W), using sharpshooter shovels. Sods were collected from the same relative elevation (approximately 50% time flooded) in healthy marsh that experiences an average 0.37-m diurnal tide range (NOAA, 2017) and were located in subtropical, mineral-based deltaic soils (Weindorf, 2008). Sods were transplanted into mesocosms (18.9 L) in the field. After collection, sods were transferred to the U.S. Geological Survey Wetland and Aquatic Research Center in Lafayette, Louisiana, United States. We trimmed sods to a uniform 20-cm soil depth, added pea gravel to the bottom of the mesocosms, and removed all fiddler crabs and snails. We drilled several holes in the side of the mesocosms, which, in combination with the pea gravel, allowed both vertical and horizontal movements of water through the mesocosm soil profile. Sods were acclimated to the mesocosms for approximately 1 month by sitting under a shade cloth with constant moisture before placement in the greenhouse facility.

The experimental greenhouse facility included four 12-m^2 greenhouses (described thoroughly in McKee & Rooth, 2008), which allowed for tight control of hydrologic and atmospheric conditions. Experimental treatments were applied using a split-plot design. At the greenhouse/whole-plot level, we varied CO_2 concentrations at ambient (~400 ppm) or elevated (~720 ppm; possible by 2100; IPCC, 2013) concentrations in two greenhouses each. Within the greenhouses, at the split-plot level, water level and inundation type were manipulated to generate nine hydrologic treatments, replicated twice in each greenhouse (Figure 1). Seven hydrologic treatments spanned the in situ tidal range, providing average water depths that occur at present or may occur by the end of the century with sea level rise (IPCC, 2013). As they are commonly used in greenhouse experiments, especially in microtidal systems, average water level in four of these treatments was kept static (−9.5 to +13.5-cm water levels compared to soil surface). To compare static treatments to more realistic field conditions, three tidal treatments that experienced 30-cm tidal inundation (one high and one low per day) were included (−12 to +9-cm average water levels compared to soil surface; 15 to 75% inundation). Two additional static treatments experienced rare hydrologic conditions outside of the average in situ tidal range (−20 and +24-cm water levels compared to soil surface), to investigate C cycling along an extended hydrologic gradient. Groups of mesocosms were placed in tanks to allow for the large volumes of water needed for treatments (Figure 1). Water levels were manipulated using aquarium pumps and drains and by controlling mesocosm elevation within tanks. In total, the whole-plot CO_2 treatment was replicated twice, with split-plot hydrologic regimes replicated 2 times in each whole-plot, for a total of 72 experimental units. This design allowed us to control for variability within greenhouses, given the limited space available. Sods were ordered by estimated initial biomass and then randomly assigned to treatments, to avoid confounding effects of initial condition.

Mesocosm salinity was set to field conditions at 20 ppt (growing season last 5 years 18.0–29.0 ppt monthly average; Coastwide Reference Monitoring System, 2017). Salinity was checked weekly, and adjustments were made with deionized water or Instant Ocean (Spectrum Brands, Inc., Blacksburg, VA, USA). Water was changed quarterly to prevent excessive algal buildup. To remove salt buildup on plant leaves, plants were lightly sprayed with deioized water biweekly. At the beginning of the experiment, all mesocosms received 2 L of 10% strength Hoagland's solution to prevent nutrient limitation. We monitored the experiment from September 2014 to November 2015. To monitor hydrologic treatment progression, pore water was collected quarterly and assayed for conductivity (YSI 3100; YSI Inc., Yellow Springs, OH, USA), pH (Orion model 420A; Thermo Fisher Scientific Inc., Waltham, MA, USA), and sulfide concentrations (modified from McKee et al., 1988). Soil redox potentials were also measured at 5 and 15 cm (Orion ORP Electrode 9179BN; Thermo Fisher Scientific Inc., Waltham, MA, USA).

2.2. Biomass Carbon Dynamics

We quantified the biomass C pool by measuring plant above- and belowground production rates and end of season biomass and converting grams of biomass to grams of C. Initial aboveground biomass was calculated by harvesting over 100 stems from the initial collection and deriving an allometric equation using stem height (biomass [g] = 0.28 * stem height [cm] − 1.07, $P < 0.01$). Dead stems were collected quarterly during the experiment, dried at 60°C, and weighed. At the end of the experiment, all aboveground biomass was harvested, dried at 60°C, and weighed. Annual aboveground biomass production was calculated as the difference between cumulative biomass (including final harvest) and initial biomass values. Root ingrowth

bags were deployed for the duration of the experiment to quantify belowground biomass production rates (Neill, 1992). Root ingrowth bags were 5 cm in diameter and were filled with mineral sediment to approximate the low organic matter marshes they were deployed in. After ingrowth bag harvest, roots and rhizomes were sorted into live and dead fractions by sieving to 2 mm and floating in water. Tissue was then dried at 60°C and weighed. End of season belowground biomass was quantified by washing soil from root material through a 2-mm sieve, drying at 60°C, and weighing. Due to the large size of mesocosms, belowground end of season biomass was not sorted into live and dead fractions. Initial belowground standing stocks were not assessed. Biomass was converted to grams C by using literature values of both above- and belowground percent C of *S. alterniflora* tissue (aboveground 42% C, belowground 38% C; Gallagher et al., 1984; McKee & Rooth, 2008). Root-to-shoot ratios were also calculated by comparing total belowground biomass to aboveground biomass following Robinson et al.'s (2010) framework (sensu Stagg, Schoolmaster, Krauss, et al., 2017), to avoid problems associated with conducting regression on ratios.

2.3. Soil Carbon Dynamics

We quantified the soil C pool by calculating soil C density from soil cores. Cores were collected at the beginning and end of the experiment using a 5-cm diameter soil corer; each 20-cm length core was dried at 60°C to constant mass and weighed. These data allowed calculation of soil moisture and bulk density via dry weight to volume (Blake & Hartge, 1986). Percent organic matter was calculated by homogenizing each dried core through a 2-mm sieve and processing a 2-g subsample using loss-on-ignition at 500°C for 5 hr, following recommendations of Wang et al. (2011). Soil organic matter was then converted to percent soil organic C (multiplied by 0.4014 for saline marsh soil in Terrebonne Basin, Louisiana; Wang et al., 2017). Percent soil organic C was multiplied by bulk density to calculate soil C density (Chmura et al., 2003) and scaled to soil C pools by multiplying C density by mesocosm-specific soil volume.

We estimated cellulose decomposition rates. The percent of tensile strength loss from cotton strips was quantified as a proxy for soil decomposition (Maltby, 1988). Cotton strips were inserted throughout the entire 20-cm soil profile at three time periods and left until approximately 65% degraded. Simultaneously, control strips were inserted into each mesocosm, immediately removed, and otherwise treated identically to test strips. After collection, cotton strips were gently washed of soil particles, dried, and cut into 2-cm-wide strips. The total force necessary to pull each strip apart was then recorded using a tensiometer (outfitted with Mecmesin BFG 1000 N; Mecmesin Limited, West Sussex, UK). To calculate percent tensile strength loss, tensile strength values for each experimental strip were divided by the average tensile strength of control strips.

2.4. Gaseous Carbon Dynamics

We quantified gaseous C cycling by measuring net ecosystem exchange of CO_2 and methane at midday during peak photosynthesis, scaling photosynthesis to total leaf area for total plant C uptake, and calculating ecosystem C respiration. Clear Plexiglas chambers (42.6 L) were placed over mesocosms (Weston et al., 2014), and 15-mL air samples were collected and stored in scintillation vials that were vacuumed during sample collection to prevent leakage. Samples were collected initially, at 30 min, and at 1-hr postchamber installation during sampling events in May, August, and November. Mesocosms were not drained for data collection, but tidal treatments were sampled at low tide to quantify maximum gas fluxes. Gas samples were analyzed using a Varian CP-3800 Gas Chromatograph (Varian Inc., Palo Alto, California, USA) for CO_2 and methane; measurable levels of nitrous oxide were not detected. Due to sample storage issues during HVAC repairs at the Wetland and Aquatic Research Center, May samples were discarded. Gas concentrations were regressed over time and fit to a linear regression, using the slope as the gas flux rates for each mesocosm (Krauss & Whitbeck, 2012).

To separate plant C uptake from net CO_2 flux, we measured photosynthesis using an LI-6400XT Portable Photosynthesis System (LI-COR Inc., Lincoln, Nebraska, USA). Photosynthesis was measured on the first fully expanded leaf on a stem in each mesocosm, allowing the leaf to equilibrate before recording data. Stomatal ratio (0.003; Maricle et al., 2009), actual chamber leaf area, and light intensity (1,200 $\mu mol * m^{-2} * s^{-1}$) were adjusted accordingly. All measurements were taken at the same time of day as gas exchange measurements, during peak photosynthesis. To scale from leaf-level to plant-level photosynthesis, total leaf area was quantified by counting the number of live leaves and multiplying by average leaf area for each mesocosm. Total leaf area was then multiplied by photosynthesis to calculate plant-level CO_2-C uptake and scaled to uptake

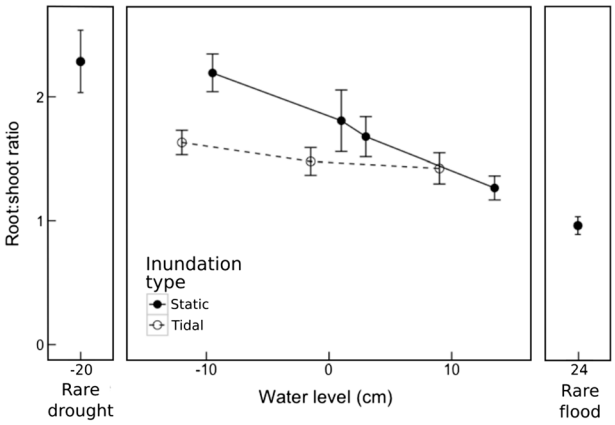

Figure 2. Root to shoot ratio response to water level and inundation type, with rare hydrologic conditions presented as comparison. No model fit, the lines are presented to visualize trend only. The values are averages ± standard error (n = 4).

per unit area (mg C * m^{-2} * h^{-1}). Finally, to estimate CO_2 respiration, CO_2 uptake was subtracted from net CO_2 flux. Net CH_4-C flux was then summed with CO_2-C respiration to calculate total C respiration (m^{-2}) for each mesocosm.

2.5. Statistical Analyses

We analyzed data using a mixed model regression framework to quantify the relationship between hydrologic regime, CO_2 concentration, and our response variables (package "nlme" in R statistical software version 3.3; Pinheiro et al., 2016; R Core Team, 2016). Mixed models allow proper accounting of nesting (Zuur et al., 2009); hydrologic regime was nested inside greenhouse as a random effect, matching our split-plot design. We did not detect any effects of greenhouse on response variables, so replicates were pooled across CO_2 treatments. When temporal effects were insignificant, data were pooled across time periods for all analyses. For all regression analyses, treatments outside of the in situ tide range were excluded from model fitting but are presented for comparison. We modeled error variance to account for heterogeneity when present (Zuur et al., 2009). Full models included CO_2 concentration (elevated or ambient), inundation type (static or tidal), water level (continuous), and all two-way interactions as fixed effects. Model selection was carried out using corrected Akaike information criterion values (due to small sample sizes) and single deletion of terms that were insignificant ($P < 0.05$). Final models were determined by using function anova. lme() between full and reduced models to ensure no significant terms were dropped. Marginally significant terms ($0.01 > P < 0.05$) were dropped if their inclusion did not improve corrected Akaike information criterion scores by at least 2. Carbon uptake, respiration, and decomposition responses were log-transformed before analysis to meet linear assumptions, and an offset was added before log-transformed analyses to remove any negative numbers. All P values for final model terms, and pseudo R^2 for final models (mixed models do not have typical R^2 due to random effects), are reported in Table S1 in the supporting information. Three outliers were removed for methane net ecosystem exchange data that were an order of magnitude larger than other samples; if present, outliers were retained for all other analyses.

3. Results

The amount of C stored in soil and biomass pools and the exchange of C between pools were altered by hydrologic regime, but not atmospheric CO_2 concentration (Table S1). Further, inundation type often affected the relationship between average water depth and response variables. With greater average flooding depth, edaphic variables indicated that our hydrologic regimes affected soil parameters as expected;

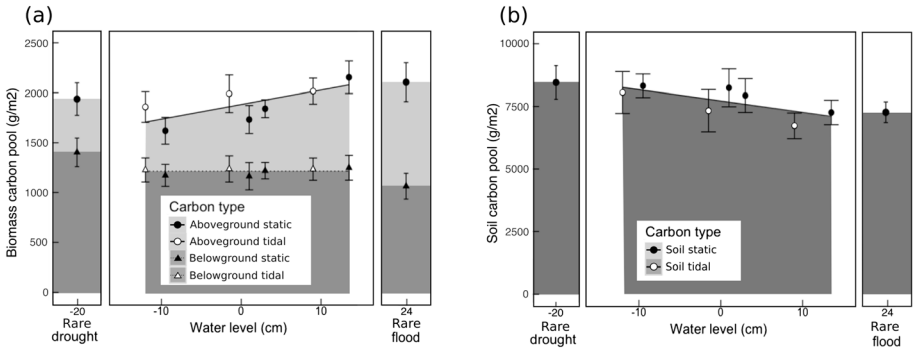

Figure 3. Total biomass (a) carbon pool and (b) soil carbon pool response to water level, with rare hydrologic conditions presented as comparison. Note change in y axis between panels. The lines represent linear mixed model fits (fixed effects: total biomass carbon [g * m^{-2}] = 1,888 + 15 * water level [cm] $P < 0.01$; belowground biomass carbon [g * m^{-2}] = 1,219 slope not significant; soil carbon pool [g * m^{-2}] = 7,777–46 * water level [cm] $P < 0.05$). The values are averages ± standard error (n = 4).

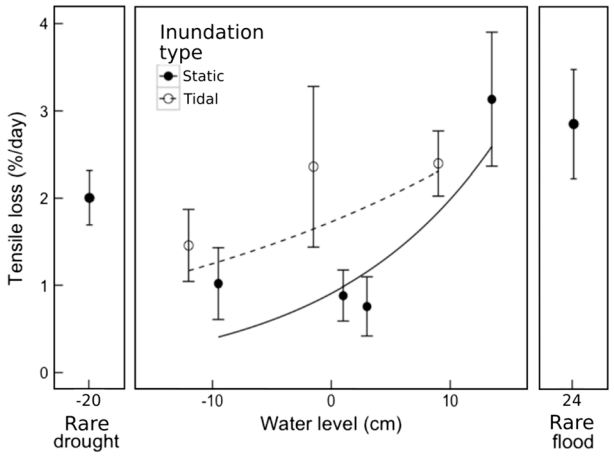

Figure 4. Cellulose decomposition response to water level and inundation type as measured by cotton strip tensile strength loss, with rare hydrologic conditions presented as comparison. The lines represent linear mixed model fits (fixed effects: Log (static tensile loss [% * d^{-1}]) = (0.005 + 0.073 * water level [cm]) − 0.1; log (tidal tensile loss [% * d^{-1}]) = (0.602 + 0.031 * water level [cm]) − 0.1; $P < 0.001$). The values are averages ± standard error ($n = 4$).

redox values for typical conditions averaged 327 mV in the least flooded treatment and −132 mV in the most flooded treatment, spanning a range of oxygen availability.

3.1. Biomass Carbon Dynamics

Greater average flooding depth doubled aboveground biomass production along our gradient from 1,043 to 2,110 g * m^{-2} * yr^{-1}. In contrast to aboveground gains, flooding did not affect total belowground production rates measured via ingrowth bags (295 g * m^{-2} * yr^{-1}) or end-of-season belowground biomass stocks (3,207 g * m^{-2}). Although total belowground production rates were unaffected by treatments, root production did increase with flooding, although tidal treatments had a muted response (Figure S1 in the supporting information). Root-to-shoot ratios indicated that with greater average flooding depth, more biomass was allocated to aboveground structures (Figure 2). Tidal treatments had lower root-to-shoot ratios than static treatments in less flooded conditions.

Greater average flooding depth enlarged the total biomass C pool by affecting aboveground stocks (Figure 3a), regardless of inundation type. For typical hydrologic regimes, an increase in water level of 10 cm increased the total C stored in the biomass pool by 150 g C * m^{-2}.

3.2. Soil Carbon Dynamics

Greater average flooding depth decreased soil C density, resulting in a smaller total soil organic C pool (Figure 3b), regardless of inundation type. For typical hydrologic regimes, an increase in water level of 10 cm decreased the soil C pool in the top 20 cm by 460 g C * m^{-2}. The soil C pool contained 3–4 times more C than the biomass C pool, and soil C pool losses outweighed biomass C pool gains (Figure 3).

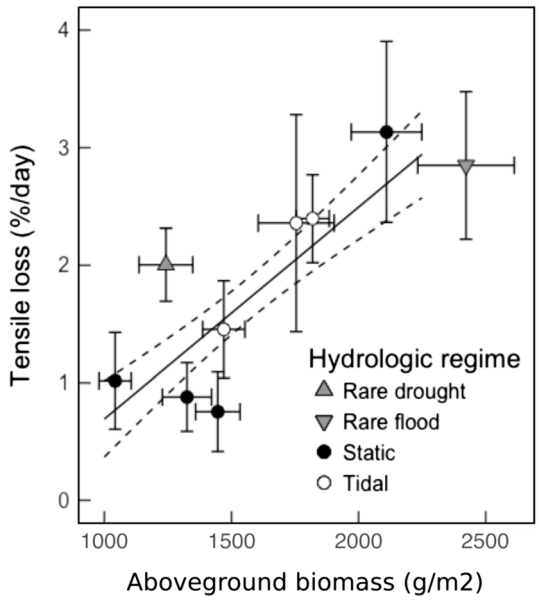

Figure 5. Average cellulose decomposition as measured by cotton strip tensile strength loss related to average aboveground plant production, with rare hydrologic conditions presented as comparison. The solid line represents linear regression fit of typical hydrologic conditions (average tensile loss [% * d^{-1}] = −1.1 + 0.0018 * average aboveground biomass [g * m^{-2}], $P < 0.0001$, $R^2 = 0.25$). The dashed line is 95% confidence interval. The values are averages of each water level treatment ± standard error ($n = 4$).

Greater average flooding depth exponentially increased decomposition rates, and tidal treatments had higher rates of decomposition than static treatments (Figure 4). Total aboveground production correlated positively with decomposition rates regardless of inundation type (Figure 5), but total belowground production did not (data not shown). Additionally, the modeled production-decomposition relationship was unable to capture the mean response of the rare drought treatment (Figure 5). Belowground root production was weakly positively correlated with decomposition rates, and tidal treatments had higher decomposition rates than static treatments (Figure S2).

3.3. Gas Carbon Dynamics

Increased CO_2 concentrations temporarily increased photosynthesis rates by 77% across all hydrologic treatments, but the effect subsided over time (Figure 6). Greater average flooding depth exponentially increased total plant C uptake; tidal treatments responded less dramatically than static treatments (Figure 7a). All treatments took in C (negative values), with the most flooded treatments taking in C at rates exceeding 750 mg C * m^{-2} * h^{-1}. Leaf number appeared to drive increased uptake with greater average flooding depth (data not shown).

Carbon dioxide dominated C gas fluxes. Nevertheless, methane emissions increased with greater average flooding depth, especially in tidal treatments (Figure S3); measurements in November exhibited the same pattern as measurements in August, but with less overall emissions (data not shown). When combined with calculated CO_2-C respiration, overall C emissions increased exponentially with greater average flooding depth; tidal treatments responded less dramatically than static treatments

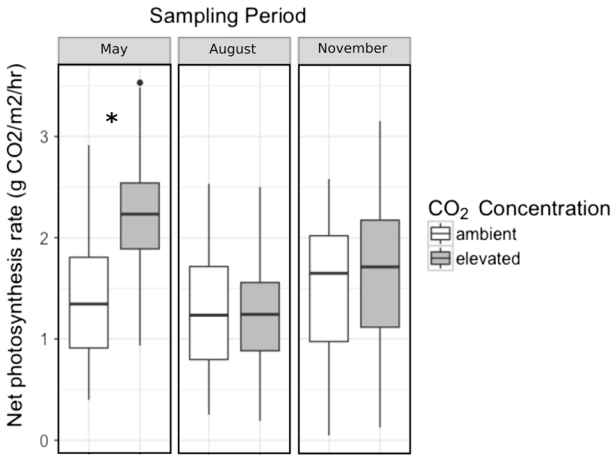

Figure 6. Net photosynthesis rate in response to CO_2 concentration, over three sample periods. The asterisks denote significant differences ($P < 0.05$) between CO_2 treatments within sample period. The boxplot boxes span the lower and upper data quartiles, with the center line the median ($n = 36$). The boxplot whiskers go out as far as 1.5 * the interquartile range. The dots are points beyond 1.5 * the interquartile range.

(Figure 7b). All treatments emitted C (positive values), with the most flooded treatments emitting C at rates exceeding 750 mg C * m^{-2} * h^{-1}. Greater average flooding depth increased both C uptake and emissions, resulting in weak net C flux patterns, especially in tidal treatments (Figure S4). Regardless of hydrologic regime, all treatments experienced net C uptake rates (negative fluxes) of 33–102 mg C * m^{-2} * h^{-1}.

4. Discussion

Sea-level rise expected before 2100 may speed soil labile C decomposition and atmospheric C exchange, decreasing the blue carbon pools of *S. alterniflora* salt marshes. Despite their common use in coastal ecosystem greenhouse manipulations, static treatments did not quantitatively respond like more realistic tidal treatments, although responses were qualitatively similar at the same average flooding depth. Additionally, an extended hydrologic gradient including rare conditions garnered insight into the mechanisms underlying decomposition rates in this system. Greenhouse studies that manipulate future climate scenarios in tidal wetlands should therefore prioritize realistic tidal hydrologic regimes if data will be used for modeling or prediction and should include treatments along extended hydrologic gradients to investigate mechanisms of C responses.

4.1. Carbon Cycling Drivers

As predicted, hydrologic regime was a strong driver of salt marsh C cycling, while CO_2 concentration did not affect C pools or cycling. We attribute this pattern to *S. alterniflora*'s use of the C-4 photosynthetic pathway, which does not strongly respond to elevated CO_2 concentrations in the absence of nutrient additions (McKee & Rooth, 2008; Sage & Kubien, 2003). Acclimation to elevated CO_2 over time may explain the temporary increase in photosynthetic rates we observed and has been shown for C-4 plants (Sage & Kubien, 2003). In a previous study, *S. alterniflora* initially increased growth in elevated CO_2 but had dampened growth responses after 4 months of treatment (Pickens, 2012).

In contrast, CO_2 fertilization work in brackish marshes of the North Atlantic supports increased growth and C gain by C-3 species on long and short timescales (Drake, 2014; Langley et al., 2009; Pastore et al., 2017). These photosynthetic pathway-specific differences in sensitivity to CO_2 concentrations may have implications for coastal wetland C cycling. Coastal wetland habitats dominated by C-4 plant species may continue to be driven by hydrology, even as CO_2 levels double from historical levels. Where a mix of C-3 and C-4 species occurs,

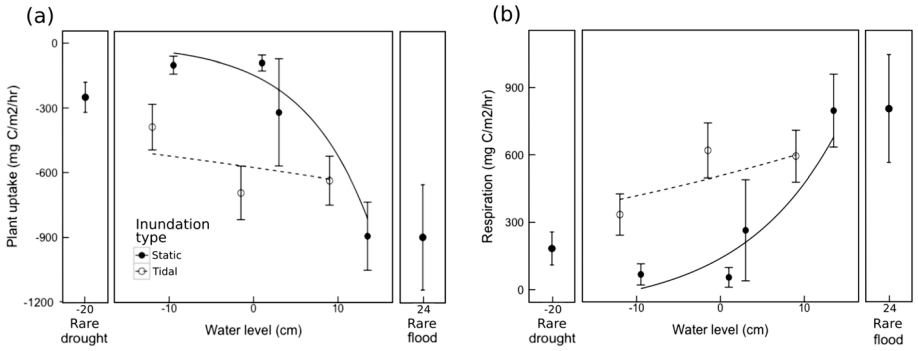

Figure 7. (a) Plant carbon uptake and (b) system respiration in response to water level and inundation type, with rare hydrologic conditions presented as comparison. The lines represent linear mixed model fits (fixed effects: Log (static plant uptake [mg C * m^{-2} * h^{-1}]) = −(4.99 + 0.13 * water level [cm]), $P < 0.0001$; log (tidal plant uptake [mg C * m^{-2} * h^{-1}]) = −(6.36 + 0.010 * water level [cm]), $P < 0.0001$; log (static system respiration [mg C * m^{-2} * h^{-1}]) = (5.48 + 0.087 * water level [cm]) − 100, $P < 0.0001$; log (tidal system respiration [mg C * m^{-2} * h^{-1}]) = (6.41 + 0.016 * water level [cm]) − 100, $P < 0.0001$). The values are averages ± standard error ($n = 4$).

shifts in species dominance over time could lead to shifts in the major drivers of C cycling in those marshes, for example, from hydrology to nitrogen availability or CO_2 concentration.

Temperature can also broadly influence carbon cycling in ecosystems (Davidson & Janssens, 2006), and average global surface temperatures will likely increase by more than 2°C with near-term climate change (IPCC, 2013). Although we could not test effects of temperature in this study, studies that manipulate carbon dioxide levels, hydrology, and temperature simultaneously are needed to fully disentangle the responses of key carbon cycling processes in salt marshes. Some work has elucidated, for example, increased decomposition rates with temperature increases in salt marshes (Kirwan & Blum, 2011; Lewis et al., 2014), a result that could exacerbate the influence of greater average water depth on decomposition rate outlined here.

4.2. Carbon Exchange

As expected, the amount of plant-mediated C exchange was related to plant production, which was strongly controlled by hydrology. Previous work has come to various conclusions regarding whether and why flooding affects decomposition in marsh habitats, from finding insignificant effects (Kirwan et al., 2013), positive effects from soil moisture (Stagg, Schoolmaster, Krauss, et al., 2017) or aboveground production (Mueller et al., 2016), and negative effects from decreased oxygen availability (Day & Megonigal, 1993). In this study, aboveground production and soil moisture increased with greater average flooding depth regardless of inundation type, while redox values decreased as expected. We therefore propose that plant production and/or soil moisture are stronger drivers of labile soil C decomposition rates than redox potential in these anaerobic systems. Mueller et al. (2016) similarly found that aboveground plant production, not flooding directly, exerts strong control on marsh soil organic matter decomposition in a brackish marsh. Although the current study was not able to detect pulses of labile C to the soil environment, our data support Mueller et al.'s (2016) conclusions and extend their findings to subtropical *S. alterniflora* saline marsh. Furthermore, we found that the production-decomposition relationship was strong except in rare drought conditions, where soil was partially oxidized. The influence of plant production on labile C decomposition may therefore be a general phenomenon in anaerobic tidal wetlands, although the direct role of sulfate-reducing and methanogenic microbial communities is understudied (Mueller et al., 2016).

Carbon gas fluxes have been related to plant production and species composition in tidal marshes (Martin & Moseman-Valtierra, 2015; Simpson et al., 2017; Sutton-Grier & Megonigal, 2011); flooding depth can also strongly influence gas flux relative contributions in wetlands (e.g., Miao et al., 2017), as in this study. Our measured methane fluxes were comparable to other salt marsh studies and were therefore low compared to brackish and fresh marsh methane emissions (e.g., Weston et al., 2014). Despite greater average flooding depth increasing gaseous C emissions, net C emissions were stable due to concomitant increases in gaseous C uptake by plant tissue. Our sampling scheme measured the potential maximum gaseous C flux as we sampled during midday conditions and at low tide in tidal treatments (Kathilankal et al., 2008). We cannot, therefore, predict overall trends in gaseous C fluxes as our samples were too infrequent to pick up on strong seasonal or diel patterns. Nonetheless, the snapshot of gaseous C fluxes presented here suggests that further research with more intensive sampling schedules should be undertaken along extended hydrologic gradients. *S. alterniflora* does have a flood stress tolerance (Mendelssohn & McKee, 1988); when this tolerance is surpassed and plant production declines, gaseous C fluxes and decomposition may decline in response. In this way, we expect that near-term climate change in this system will induce temporary increases in the amount of C exchange, with a concomitant decrease as plant stress thresholds are exceeded.

4.3. Carbon Pools

Aboveground production did not follow the expected unimodal relationship with hydrology (e.g., Morris et al., 2002). Instead, we found a positive linear relationship between aboveground C pool and flooding. Our aboveground production values compare well to studies on *S. alterniflora* on the subtropical Gulf Coast (Kirwan et al., 2009; Stagg, Schoolmaster, Piazza, et al., 2017). We observed a marginal increase in belowground root production and no response in total belowground production in response to greater average flooding depth; this is in contrast to previous studies that have shown decreases in *S. alterniflora* belowground biomass in response to increased flooding (Snedden et al., 2015; Voss et al., 2013; Watson et al., 2017). Other marsh species also typically respond strongly to flooding in biomass production above- and belowground (e.g., Janousek et al., 2016; Kirwan & Guntenspergen, 2012). We are confident that our

20-cm soil depth captured realistic belowground responses in this species, especially for live roots (Darby & Turner, 2008). *S. alterniflora* may need more intense and long-lasting stressful conditions than experienced during this study before plant responses affect biomass C pools. Ultimately, our greenhouse manipulations may be especially applicable to initial responses of salt marshes to near-term climate change and stressor interactions, while field studies may be necessary to elucidate longer term biomass C pool responses.

Soil C pools decreased linearly with greater average flooding depth, a product of enhanced decomposition. Some C also undoubtedly left the soil dissolved in water; this unmeasured pool of C may play an important role in C losses with climate change for wetlands (e.g., Freeman et al., 2004). Heightened decomposition rates are therefore not the only potential route for the C loss we observed. Our overall soil C density across treatments is similar but slightly lower than values reported for Terrebonne Basin, LA (0.049 g * cm^{-3} [15 cm soil depth] in Hinson et al., 2017; 0.034–0.040 g * cm^{-3} present study). Our range of soil C pools also compares well to other estimates in salt marsh systems (78 ± 6 Mg * ha^{-1} [20 cm soil depth] in Chmura et al., 2003; 68–84 Mg * ha^{-1} present study). Most of the C in marshes (and vegetated habitats generally; Post et al., 1982) is stored in the soil, which can sequester C long term (Chmura et al., 2003). Losses in soil C are therefore especially relevant for blue carbon pools, as opposed to aboveground biomass which is largely recycled and decomposed annually (Dai & Wiegert, 1996; Morris & Haskin, 1990). With flooding equivalent to relative sea level rise that coastal Louisiana marshes will experience before 2050 (10 cm; Gonzáles & Törnqvist, 2006; IPCC, 2013), the net C pool measured here would decrease by 313 g * m^{-2}. Losses in the soil organic C pool more than offset modest gains in the aboveground biomass C pool, with predicted net losses from 10 cm of relative sea level rise representing approximately 4% of the average C pool. This is a disconcerting decrease in the often-touted blue carbon storage capacity of salt marshes, especially as we expect our biomass C pool increases with flooding to become less positive as flooding conditions continue long term.

4.4. Experimental Considerations

Realistic tidal treatments significantly differed from static treatments at the same average water depth for almost all responses (Table S1). Static treatments have been commonly used in wetland research and did respond in the same general qualitative manner as more realistic tidal treatments. Static treatments therefore can inform response trajectories over hydrologic gradients. However, to more accurately model and predict quantitative responses such as decomposition rates, net C flux rates, and other key processes, tidal treatments were necessary. This finding is especially important for microtidal marshes like the Northern Gulf of Mexico, where meteorologically driven and weak tidal forcing make static treatments seemingly realistic. We expect that static treatments will be even less predictive in marshes with larger tidal ranges.

By working along an extended hydrologic gradient, we gained insight into the potential mechanisms underlying decomposition rates in salt marshes. We hypothesize that decomposition drivers shift from plant production in anaerobic conditions to oxygen availability in rare drought conditions; this response is critical to understand as high decomposition rates in drought conditions may trigger large-scale respiration of previously stored C pools. To better understand decomposition rates during rare conditions, mechanistic hypotheses must be put forward for blue carbon systems (sensu Stagg, Schoolmaster, Krauss, et al., 2017). As measuring rare conditions in the field is difficult due to their stochastic nature, manipulative greenhouse experiments are imperative to better understand mechanistic responses of C cycling. As blue carbon systems are crucial habitats in mitigating the effects of climate change globally, understanding feedbacks between C cycling, climate change, and rare conditions is paramount.

4.5. Conclusion

This study presents evidence that changes in environmental gradients associated with near-term climate change can strongly influence plant-mediated C cycling and that realistic tidal treatments along extended hydrologic gradients can better inform our understanding of C cycling mechanisms. This research warrants investigation of other blue carbon systems to determine how their C cycling may shift with near-term climate change. Future experiments with other key drivers, such as temperature, will be needed for a robust understanding of C cycling. By altering plant-mediated C cycling, climate change within the next century has the potential to decrease the amount of C in soil C pools by increasing decomposition rates and other processes, at least temporarily. For blue carbon systems such as salt marshes, this could hamper C sequestration and storage and influence habitat persistence in a dynamic landscape.

Acknowledgments
The authors would like to acknowledge assistance in data collection from the University of Louisiana Coastal Plant Ecology Lab (L. Feher, M. McCoy, T. Sloey, J. Willis, and E. Yando), ULL undergraduate assistants (L. Delcambre, G. Griffard, J. McLeod, and B. Miller), employees at the Wetland and Aquatic Research Center (E. Bergeron, N. Cormier, A. Hartmann, L. Hebert, C. Hall, L. Leonpacher, J. McCoy, R. Moss, K. Peterson, J. Reynolds, and W. Vervaeke), T. Blanchard at Louisiana State University, K. Jones, and A. Mayfield. S. Duke-Sylvester was helpful in sorting out the statistical framework. We thank E. Yando and several anonymous reviewers for insightful comments on the manuscript. Data supporting this publication can be found at Science Base (doi: 10.5066/F7NK3D7M). Funding was provided by the Louisiana Board of Regents, ULL Graduate Student Organization, the Institute for Coastal and Water Research, and the U.S. Geological Survey Climate and Land Use Change R&D and LandCarbon Programs. Any use of trade, firm, or product names is for descriptive purposes only and does not imply endorsement by the U.S. Government.

References

Beisner, B. E., Haydon, D. T., & Cuddington, K. (2003). Alternative stable states in ecology. *Frontiers in Ecology and the Environment*, *1*(7), 376–382. https://doi.org/10.1890/1540-9295(2003)001[0376:ASSIE]2.0.CO;2

Blake, G., & Hartge, K. (1986). *Methods of soil analysis: Part 1—Physical and mineralogical methods* (pp. 377–382). Madison, WI: Soil Science Society of America, Inc.

Bridgham, S. D., Megonigal, J. P., Keller, J. K., Bliss, N. B., & Trettin, C. (2006). The carbon balance of North American wetlands. *Wetlands*, *26*(4), 889–916. https://doi.org/10.1672/0277-5212(2006)26[889:TCBONA]2.0.CO;2

Cherry, J. A., McKee, K. L., & Grace, J. B. (2009). Elevated CO_2 enhances biological contributions to elevation change in coastal wetlands by offsetting stressors associated with sea-level rise. *Journal of Ecology*, *97*(1), 67–77. https://doi.org/10.1111/j.1365-2745.2008.01449.x

Chmura, G. L., Anisfeld, S. C., Cahoon, D. R., & Lynch, J. C. (2003). Global carbon sequestration in tidal, saline wetland soils. *Global Biogeochemical Cycles*, *17*(4), 1111. https://doi.org/10.1029/2002GB001917

Coastwide Reference Monitoring System (2017). Data viewer for CRMS site 0292. Retrieved from https://www.lacoast.gov/intChart/Default.aspx? Stat=CRMS0292-H01. (Accessed March 2017).

Dai, T., & Wiegert, R. G. (1996). Ramet population dynamics and net aerial primary productivity of Spartina alterniflora. *Ecology*, *77*(1), 276–288. https://doi.org/10.2307/2265677

Darby, F. A., & Turner, R. E. (2008). Below-and aboveground biomass of Spartina alterniflora: Response to nutrient addition in a Louisiana salt marsh. *Estuaries and Coasts*, *31*(2), 326–334. https://doi.org/10.1007/s12237-008-9037-8

Davidson, E. A., & Janssens, I. A. (2006). Temperature sensitivity of soil carbon decomposition and feedbacks to climate change. *Nature*, *440*(7081), 165–173. https://doi.org/10.1038/nature04514

Day, F. P., & Megonigal, J. P. (1993). The relationship between variable hydroperiod, production allocation, and belowground organic turnover in forested wetlands. *Wetlands*, *13*(2), 115–121. https://doi.org/10.1007/BF03160871

Drake, B. G. (2014). Rising sea level, temperature, and precipitation impact plant and ecosystem responses to elevated CO_2 on a Chesapeake Bay wetland: Review of a 28-year study. *Global Change Biology*, *20*(11), 3329–3343. https://doi.org/10.1111/gcb.12631

Duarte, C. M., Losada, I. J., Hendriks, I. E., Mazarrasa, I., & Marbà, N. (2013). The role of coastal plant communities for climate change mitigation and adaptation. *Nature Climate Change*, *3*(11), 961–968. https://doi.org/10.1038/nclimate1970

Erickson, J. E., Megonigal, J. P., Peresta, G., & Drake, B. G. (2007). Salinity and sea level mediate elevated CO_2 effects on C3-C4 plant interactions and tissue nitrogen in a Chesapeake Bay tidal wetland. *Global Change Biology*, *13*(1), 202–215. https://doi.org/10.1111/j.1365-2486.2006.01285.x

Freeman, C., Fenner, N., Ostle, N. J., Kang, H., Dowrick, D. J., Reynolds, B., et al. (2004). Export of dissolved organic carbon from peatlands under elevated carbon dioxide levels. *Nature*, *430*(6996), 195–198. https://doi.org/10.1038/nature02707

Gallagher, J. L., Wolf, P. L., & Pfeiffer, W. J. (1984). Rhizome and root growth rates and cycles in protein and carbohydrate concentrations in Georgia Spartina alterniflora Loisel. Plants. *American Journal of Botany*, *71*(2), 165–169. https://doi.org/10.1002/j.1537-2197.1984.tb12500.x

Gonzáles, J. L., & Törnqvist, T. E. (2006). Coastal Louisiana in crisis: Subsidence or sea level rise? *Eos*, *87*(45), 493–498. https://doi.org/10.1029/2006EO450001

Hinson, A. L., Feagin, R. A., Eriksson, M., Najjar, R. G., Herrmann, M., Bianchi, T. S., et al. (2017). The spatial distribution of soil organic carbon in tidal wetland soils of the continental United States. *Global Change Biology*, *23*(12), 5468–5480. https://doi.org/10.1111/gcb.13811

Hopkinson, C. S., Cai, W. J., & Hu, X. (2012). Carbon sequestration in wetland dominated coastal systems—A global sink of rapidly diminishing magnitude. *Current Opinion in Environmental Sustainability*, *4*(2), 186–194. https://doi.org/10.1016/j.cosust.2012.03.005

IPCC (2013). *Climate change 2013: The physical science basis. Contribution of working group I to the fifth assessment report of the Intergovernmental Panel on Climate Change*. Cambridge, UK: Cambridge University Press.

Janousek, C. N., Buffington, K. J., Thorne, K. M., Guntenspergen, G. R., Takekawa, J. Y., & Dugger, B. D. (2016). Potential effects of sea-level rise on plant productivity: Species-specific responses in Northeast Pacific tidal marshes. *Marine Ecology Progress Series*, *548*, 111–125. https://doi.org/10.3354/meps11683

Jones, S. F., Stagg, C. L., Krauss, K. W., & Hester, M. W. (2018). Salt marsh carbon dynamics under altered hydrologic regimes and elevated CO_2 conditions, Louisiana, USA (2014-2015): U.S. Geological Survey data release. https://doi.org/10.5066/F7NK3D7M

Kathilankal, J. C., Mozdzer, T. J., Fuentes, J. D., D'Odorico, P., McGlathery, K. J., & Zieman, J. C. (2008). Tidal influences on carbon assimilation by a salt marsh. *Environmental Research Letters*, *3*(4), 044010. https://doi.org/10.1088/1748-9326/3/4/044010

Kirwan, M. L., & Blum, L. K. (2011). Enhanced decomposition offsets enhanced productivity and soil carbon accumulation in coastal wetlands responding to climate change. *Biogeosciences*, *8*(4), 987–993. https://doi.org/10.5194/bg-8-987-2011

Kirwan, M. L., & Guntenspergen, G. R. (2012). Feedbacks between inundation, root production, and shoot growth in a rapidly submerging brackish marsh. *Journal of Ecology*, *100*(3), 764–770. https://doi.org/10.1111/j.1365-2745.2012.01957.x

Kirwan, M. L., Guntenspergen, G. R., & Morris, J. T. (2009). Latitudinal trends in Spartina alterniflora productivity and the response of coastal marshes to global change. *Global Change Biology*, *15*(8), 1982–1989. https://doi.org/10.1111/j.1365-2486.2008.01834.x

Kirwan, M. L., Langley, J., Guntenspergen, G. R., & Megonigal, J. (2013). The impact of sea-level rise on organic matter decay rates in Chesapeake Bay brackish tidal marshes. *Biogeosciences*, *10*(3), 1869–1876. https://doi.org/10.5194/bg-10-1869-2013

Krauss, K. W., & Whitbeck, J. L. (2012). Soil greenhouse gas fluxes during wetland forest retreat along the lower Savannah River, Georgia (USA). *Wetlands*, *32*(1), 73–81. https://doi.org/10.1007/s13157-011-0246-8

Lal, R. (2004). Soil carbon sequestration impacts on global climate change and food security. *Science*, *304*(5677), 1623–1627. https://doi.org/10.1126/science.1097396

Langley, J. A., McKee, K. L., Cahoon, D. R., Cherry, J. A., & Megonigal, J. P. (2009). Elevated CO2 stimulates marsh elevation gain, counterbalancing sea-level rise. *Proceedings of the National Academy of Sciences*, *106*(15), 6182–6186. https://doi.org/10.1073/pnas.0807695106

Langley, J. A., & Megonigal, J. P. (2010). Ecosystem response to elevated CO2 levels limited by nitrogen-induced plant species shift. *Nature*, *466*(7302), 96–99. https://doi.org/10.1038/nature09176

Langley, J. A., Mozdzer, T. J., Shepard, K. A., Hagerty, S. B., & Megonigal, J. P. (2013). Tidal marsh plant responses to elevated CO2, nitrogen fertilization, and sea level rise. *Global Change Biology*, *19*(5), 1495–1503. https://doi.org/10.1111/gcb.12147

Lewis, D. B., Brown, J. A., & Jimenez, K. L. (2014). Effects of flooding and warming on soil organic matter mineralization in Avicennia germinans mangrove forests and Juncus roemerianus salt marshes. *Estuarine, Coastal and Shelf Science*, *139*, 11–19. https://doi.org/10.1016/j.ecss.2013.12.032

Maltby, E. (1988). Cotton Strip Assay: An Index of Decomposition in Soils. 140–154. Institute of Terrestrial Ecosystems, UK.

Maricle, B. R., Koteyeva, N. K., Voznesenskaya, E. V., Thomasson, J. R., & Edwards, G. E. (2009). Diversity in leaf anatomy, and stomatal distribution and conductance, between salt marsh and freshwater species in the C4 genus Spartina (Poaceae). *New Phytologist*, *184*(1), 216–233. https://doi.org/10.1111/j.1469-8137.2009.02903.x

Martin, R. M., & Moseman-Valtierra, S. (2015). Greenhouse gas fluxes vary between Phragmites australis and native vegetation zones in coastal wetlands along a salinity gradient. *Wetlands*, *35*(6), 1021–1031. https://doi.org/10.1007/s13157-015-0690-y

McKee, K. L., Mendelssohn, I. A., & Hester, M. W. (1988). Reexamination of pore water sulfide concentrations and redox potentials near the aerial roots of Rhizophora mangle and Avicennia germinans. *American Journal of Botany*, *75*(9), 1352–1359. https://doi.org/10.1002/j.1537-2197.1988.tb14196.x

McKee, K. L., Mendelssohn, I. A., & Materne, M. D. (2004). Acute salt marsh dieback in the Mississippi River deltaic plain: A drought-induced phenomenon? *Global Ecology and Biogeography*, *13*(1), 65–73. https://doi.org/10.1111/j.1466-882X.2004.00075.x

McKee, K. L., & Rooth, J. E. (2008). Where temperate meets tropical: Multi-factorial effects of elevated CO2, nitrogen enrichment, and competition on a mangrove-salt marsh community. *Global Change Biology*, *14*(5), 971–984. https://doi.org/10.1111/j.1365-2486.2008.01547.x

Mcleod, E., Chmura, G. L., Bouillon, S., Salm, R., Björk, M., Duarte, C. M., et al. (2011). A blueprint for blue carbon: Toward an improved understanding of the role of vegetated coastal habitats in sequestering CO2. *Frontiers in Ecology and the Environment*, *9*(10), 552–560. https://doi.org/10.1890/110004

Mendelssohn, I. A., & McKee, K. L. (1988). Spartina alterniflora die-back in Louisiana: Time-course investigation of soil waterlogging effects. *Journal of Ecology*, *76*(2), 509–521. https://doi.org/10.2307/2260609

Miao, G., Noormets, A., Domec, J. C., Fuentes, M., Trettin, C. C., Sun, G., & King, J. S. (2017). Hydrology and microtopography control carbon dynamics in wetlands: Implications in partitioning ecosystem respiration in a coastal plain forested wetland. *Agricultural and Forest Meteorology*, *247*, 343–355. https://doi.org/10.1016/j.agrformet.2017.08.022

Mitsch, W. J., Bernal, B., Nahlik, A. M., Mander, Ü., Zhang, L., Anderson, C. J., & Brix, H. (2013). Wetlands, carbon, and climate change. *Landscape Ecology*, *28*(4), 583–597. https://doi.org/10.1007/s10980-012-9758-8

Morris, J. T., & Haskin, B. (1990). A 5-yr record of aerial primary production and stand characteristics of Spartina alterniflora. *Ecology*, *71*(6), 2209–2217. https://doi.org/10.2307/1938633

Morris, J. T., Sundareshwar, P., Nietch, C. T., Kjerfve, B., & Cahoon, D. (2002). Responses of coastal wetlands to rising sea level. *Ecology*, *83*(10), 2869–2877. https://doi.org/10.1890/0012-9658(2002)083[2869:ROCWTR]2.0.CO;2

Mueller, P., Jensen, K., & Megonigal, J. P. (2016). Plants mediate soil organic matter decomposition in response to sea level rise. *Global Change Biology*, *22*(1), 404–414. https://doi.org/10.1111/gcb.13082

Neill, C. (1992). Comparison of soil coring and ingrowth methods for measuring belowground production. *Ecology*, *73*(5), 1918–1921. https://doi.org/10.2307/1940044

NOAA (2017). Tides & currents—Station info. for Port Fourchon, Belle Pass, LA - Station ID: 8762075. Retrieved from https://tidesandcurrents.noaa.gov/stationhome. html? id=8762075. (Accessed March 2017).

Pan, Y., Birdsey, R. A., Fang, J., Houghton, R., Kauppi, P. E., Kurz, W. A., & Hayes, D. (2011). A large and persistent carbon sink in the world's forests. *Science*, *333*(6045), 988–993. https://doi.org/10.1126/science.1201609

Pastore, M. A., Megonigal, J. P., & Langley, J. A. (2017). Elevated CO_2 and nitrogen addition accelerate net carbon gain in a brackish marsh. *Biogeochemistry*, *133*(1), 73–87. https://doi.org/10.1007/s10533-017-0312-2

Pickens, C. (2012). Influence of climate change on the ecophysiology and restoration ecology of black mangrove (Avicennia germinans (L.)). Dissertation at University of Louisiana at Lafayette, Lafayette, LA.

Pinheiro, J., Bates, D., DebRoy, S., Sarkar, D., & R Core Team (2016). nlme: Linear and nonlinear mixed effects models.

Post, W. M., Emanuel, W. R., Zinke, P. J., & Stangenberger, A. G. (1982). Soil carbon pools and world life zones. *Nature*, *298*(5870), 156–159. https://doi.org/10.1038/298156a0

R Core Team (2016). R: A language and environment for statistical computing Vienna, Austria.

Reddy, K., & DeLaune, R. (2008). *Biogeochemistry of wetlands: Science and applications*. Boca Raton, FL: CRC Press. https://doi.org/10.1201/9780203491454

Reed, D. J. (1995). The response of coastal marshes to sea-level rise: Survival or submergence? *Earth Surface Processes and Landforms*, *20*(1), 39–48. https://doi.org/10.1002/esp.3290200105

Robinson, D., Davidson, H., Trinder, C., & Brooker, R. (2010). Root-shoot growth responses during interspecific competition quantified using allometric modelling. *Annals of Botany*, *106*(6), 921–926. https://doi.org/10.1093/aob/mcq186

Sage, R. F., & Kubien, D. S. (2003). Quo vadis C4? An ecophysiological perspective on global change and the future of C4 plants. *Photosynthesis Research*, *77*(2-3), 209–225. https://doi.org/10.1023/A:1025882003661

Simpson, L. T., Osborne, T. Z., Duckett, L. J., & Feller, I. C. (2017). Carbon storages along a climate induced coastal wetland gradient. *Wetlands*, 1–13.

Snedden, G. A., Cretini, K., & Patton, B. (2015). Inundation and salinity impacts to above- and belowground productivity in Spartina patens and Spartina alterniflora in the Mississippi River deltaic plain: Implications for using river diversions as restoration tools. *Ecological Engineering*, *81*, 133–139. https://doi.org/10.1016/j.ecoleng.2015.04.035

Stagg, C. L., Schoolmaster, D. R., Krauss, K. W., Cormier, N., & Conner, W. H. (2017). Causal mechanisms of soil organic matter decomposition: Deconstructing salinity and flooding impacts in coastal wetlands. *Ecology*, *98*(8), 2003–2018. https://doi.org/10.1002/ecy.1890

Stagg, C. L., Schoolmaster, D. R., Piazza, S. C., Snedden, G., Steyer, G. D., Fischenich, C. J., & McComas, R. W. (2017). A landscape-scale assessment of above- and belowground primary production in coastal wetlands: Implications for climate change-induced community shifts. *Estuaries and Coasts*, *40*(3), 856–879. https://doi.org/10.1007/s12237-016-0177-y

Sutton-Grier, A. E., & Megonigal, J. P. (2011). Plant species traits regulate methane production in freshwater wetland soils. *Soil Biology and Biochemistry*, *43*(2), 413–420. https://doi.org/10.1016/j.soilbio.2010.11.009

Thompson, R. M., Beardall, J., Beringer, J., Grace, M., & Sardina, P. (2013). Means and extremes: Building variability into community-level climate change experiments. *Ecology Letters*, *16*(6), 799–806. https://doi.org/10.1111/ele.12095

Voss, C. M., Christian, R. R., & Morris, J. T. (2013). Marsh macrophyte responses to inundation anticipate impacts of sea-level rise and indicate ongoing drowning of North Carolina marshes. *Marine Biology*, *160*(1), 181–194. https://doi.org/10.1007/s00227-012-2076-5

Wang, H., Piazza, S. C., Sharp, L. A., Stagg, C. L., Couvillion, B. R., Steyer, G. D., & McGinnis, T. E. (2017). Determining the spatial variability of wetland soil bulk density, organic matter, and the conversion factor between organic matter and organic carbon across coastal Louisiana, U.S.A. *Journal of Coastal Research*, *33*(3), 507–517.

Wang, Q., Li, Y., & Wang, Y. (2011). Optimizing the weight loss-on-ignition methodology to quantify organic and carbonate carbon of sediments from diverse sources. *Environmental Monitoring and Assessment*, *174*(1-4), 241–257. https://doi.org/10.1007/s10661-010-1454-z

Watson, E. B., Wigand, C., Davey, E. W., Andrews, H. M., Bishop, J., & Raposa, K. B. (2017). Wetland loss patterns and inundation-productivity relationships prognosticate widespread salt marsh loss for southern New England. *Estuaries and Coasts*, *40*(3), 662–681. https://doi.org/10.1007/s12237-016-0069-1

Weindorf, D. C. (2008). An update of the field guide to Louisiana soil classification, bulletin no. 669. Louisiana State University Ag Center, Baton Rouge, LA.

Weston, N. B., Neubauer, S. C., Velinsky, D. J., & Vile, M. A. (2014). Net ecosystem carbon exchange and the greenhouse gas balance of tidal marshes along an estuarine salinity gradient. *Biogeochemistry*, *120*(1-3), 163–189. https://doi.org/10.1007/s10533-014-9989-7

Zedler, J. B., Covin, J., Nordby, C., Williams, P., & Boland, J. (1986). Catastrophic events reveal the dynamic nature of salt-marsh vegetation in southern California. *Estuaries and Coasts*, *9*(1), 75–80. https://doi.org/10.2307/1352195

Zuur, A., Ieno, E., Walker, N., Saveliev, A., & Smith, G. (2009). *Mixed effects models and extensions in ecology*. New York: Spring Science and Business Media.